Scattering models of conduction around an antidot in a magnetic field

George Kirczenow
Department of Physics, Simon Fraser University, Burnaby, British Columbia, Canada V5A 1S6 and Institute for Microstructural Sciences, National Research Council, Ottawa, Canada K1A 0R6*
(Received 11 November 1993)

Magnetotransport through a pair of parallel ballistic conducting channels separated by an antidot is studied theoretically using models with magnetic edge states linked by unitary scattering matrices. Analytic solutions of the models are presented. A model is identified that exhibits abrupt phase shifts of magnetoconductance oscillations and beatlike conductance features similar to those that have recently been observed experimentally. The effect of temperature on the beatlike structures is discussed. Another possible explanation for the experimentally observed phase shifts is also mentioned.

I. INTRODUCTION

Following the discovery[1] and explanation[1,2] of conductance quantization of ballistic constrictions in semiconductor heterostructures, there has been much interest in quantum transport in more general ballistic nanostructures.[3] Systems of parallel ballistic conductors connecting a pair of electron reservoirs are in this category. Experimental[4-6] and theoretical[7-10] studies of them have revealed a number of interesting phenomena: In the absence of magnetic fields, they exhibit additive parallel conductances,[8,4,6] and possibly energy-level locking,[4,10] although the latter effect is controversial.[11] When a magnetic field is applied, Aharonov-Bohm[12]-like conductance oscillations appear[4,5,9] because of the multiply connected geometry.

Very recent progress in nanofabrication technology has made it possible to study the parallel conduction experimentally in a more controlled way, and a number of additional interesting effects have been observed:[13-16] At high magnetic fields, a magnetic edge state bound to the "antidot" separating the parallel conducting channels, becomes sufficiently weakly coupled to the rest of the system that it exhibits pronounced charging effects.[13-15] These are related to the Coulomb blockade,[17] and their presence in a completely open geometry is interesting. However, certain phenomena observed at lower magnetic fields have been interpreted in terms of noninteracting electrons. These include abrupt phase changes[14,15] and beatlike features[16] that are observed in the magneto-oscillations of the conductance. Abrupt period changes of the conductance oscillations that are also observed at the lower fields have been interpreted as effects of edge-state formation and its influence on the local Fermi level.[16] Neither the high-field nor the lower-field behavior is completely understood at present. Thus, it is important to establish precisely what noninteracting electron theories predict about these systems. One way to do this is by computer simulations, using numerical lattice Green's-function techniques.[18,19] This approach has very recently been applied to the problem of an antidot between a pair of conducting channels.[19] However, it is also useful to understand the physics in terms of simpler models and their analytic solutions. A suitable approach is to model conduction in terms of magnetic edge states[20] linked by unitary scattering matrices.[21-24] It has previously been used to study transport in Hall bars with resonant defects,[22,24] quantum wire junctions,[23,24] quantum dots,[25] and quantum dot arrays.[26] This approach relies on the unitarity of scattering matrices (an exact property), and good agreement with key results of much more complicated numerical studies can often be achieved.[23,27]

In the present paper, this approach is applied to the problem of the parallel ballistic conductors.[28] In Secs. II and III the edge-state models of these systems that have been proposed previously are analyzed. It is found that they cannot explain the abrupt phase changes of the magnetoconductance oscillations and beatlike features that have been recently observed. An improved model is presented, together with its analytic solution, in Sec. IV. In Sec. V, it is shown that this model exhibits abrupt phase changes and beatlike features similar to those that are observed. The temperature dependence of the beats and how it is affected by the magnetic field are briefly discussed. Some limitations of the model and a possible alternative explanation of the phase changes are mentioned in Sec. VI.

II. THE SIMPLEST EDGE-STATE CONFIGURATIONS

The simplest models of edge-state transport through a pair of conducting channels arranged in parallel are shown schematically in Figs. 1(a) and 1(b). Electrons are excluded from the black areas. The center black region is the antidot. The measured electric current flows in each case between the two conducting regions (white areas) located above and below the antidot. The solid lines represent the electron edge states, while the dashed lines indicate scattering processes between the edge states. Figure 1(a) shows the case where the edge states are transmitted through the two conducting channels with some reflection (backscattering of an electron from L to R or from R to L) happening because of the scattering between edge states occurring at a and b. Figure 1(b) depicts the edge states being reflected at the channel openings with some transmissions through the channels

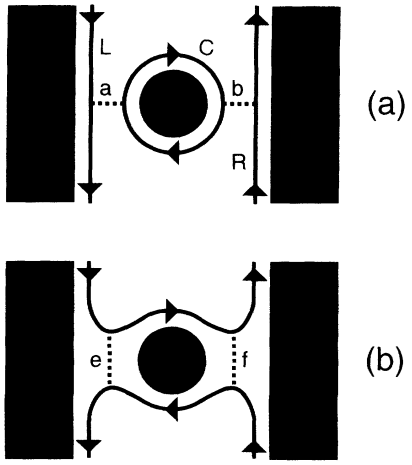

FIG. 1. The simplest models of a pair of parallel conducting channels. There is only a single participating magnetic edge state (solid line) at each boundary between the electron gas (white) and depleted regions (black). Dashed lines denote scattering between different edge states. The electric current flows between reservoirs located at the top and bottom of each figure. (a) the edge states are transmitted through the conducting channels, with some reflection occurring due to mixing between edge states at a and b. (b) The edge states are reflected at the mouths of the conducting channels, with some transmission occurring due to mixing at e and f.

occurring because of the scattering processes e and f. A switch from resonant reflection in the configuration of Fig. 1(a) to resonant transmission in Fig. 1(b) has been suggested as a possible explanation of the abrupt π phase changes that are observed[14,15] in the magnetoconductance oscillations of the antidot systems. Such a switch is not found in the theory described here.

A feature of the present theory is that although Figs. 1(a) and 1(b) may appear different physically, the same mathematics describes both of them. That is, the cases of weak and strong transmission through the constrictions simply correspond to different values of the scattering matrix elements. In the treatment given below, the notation refers to Fig. 1(a); however, the results are equally applicable to Fig. 1(b). The objective is to calculate the quantum transmission probability of an electron through the pair of parallel channels and hence the two-terminal conductance of the system.[29]

In Fig. 1(a), let the three edge states present be labeled L, R, and C as shown. Let the current amplitude of edge state X that is incident on (flowing out from) scattering region y be J^I_{Xy} (J^O_{Xy}). Then the scattering between the edge states at a and b can be written as

$$J^O_{La}=U^a_{LL}J^I_{La}+U^a_{LC}J^I_{Ca} , \tag{1}$$

$$J^O_{Ca}=U^a_{CL}J^I_{LA}+U^a_{CC}J^I_{Ca} , \tag{2}$$

$$J^O_{Cb}=U^b_{CR}J^I_{Rb}+U^b_{CC}J^I_{Cb} , \tag{3}$$

$$J^O_{Rb}=U^b_{RR}J^I_{Rb}+U^b_{RC}J^I_{Cb} , \tag{4}$$

where U^a and U^b are the unitary scattering matrices describing the scattering regions a and b. Writing them in the form

$$U^y_{XX'}=u^y_{XX'}e^{i\theta^y_{XX'}} , \tag{5}$$

where $u^y_{XX'}$ is real and positive, unitarity implies that the scattering phase shifts $\theta^y_{XX'}$ obey

$$\exp[i(\theta^y_{XX}+\theta^y_{X'X'}-\theta^y_{XX'}-\theta^y_{X'X})]=-1 , \tag{6}$$

and that

$$u^y_{XX'}=u^y_{X'X}=\sqrt{1-(u^y_{XX})^2}=\sqrt{1-(u^y_{X'X'})^2} , \tag{7}$$

if X and X' are *different* edge states.

Edge state C accumulates a phase φ^C_{ba} in propagating from scattering region a to scattering region b and a phase φ^C_{ab} in propagating from b to a. Thus,

$$J^I_{Ca}=e^{i\varphi^C_{ab}}J^O_{Cb} , \tag{8}$$

$$J^I_{Cb}=e^{i\varphi^C_{ba}}J^O_{Ca} . \tag{9}$$

The transmission probability of an electron at the Fermi energy through the pair of parallel conducting channels is given by

$$T=\left|\frac{J^O_{La}}{J^I_{La}}\right|^2 , \tag{10}$$

if $J^I_{Rb}=0$, i.e., it is the probability that an electron entering the system in edge state L at the upper left in Fig. 1(a), exits via edge state L at the lower left.

Equation (10) can be evaluated by solving (1)–(4), using (5)–(9). This yields

$$T=1-\frac{(1-t_a^2)(1-t_b^2)}{t_a^2t_b^2-2t_at_b\cos(\Phi^C)+1} . \tag{11}$$

Here

$$t_a=u^a_{LL}=u^a_{CC} \tag{12}$$

and

$$t_b=u^b_{RR}=u^b_{CC} \tag{13}$$

are the moduli of the transmission amplitudes of the two individual conducting channels (t_a^2 and t_b^2 are the corresponding transmission probabilities) and

$$\Phi^C=\varphi^C_{ba}+\theta^a_{CC}+\varphi^C_{ab}+\theta^b_{CC} \tag{14}$$

is the phase accumulated by the edge state C in a complete orbit of the antidot, including the phase shifts θ^a_{CC} and θ^b_{CC} that are acquired in the scattering processes a and b.

In Fig. 1(a), the orbit C comes into resonance when the phase accumulated by an electron going around it once is an integer multiple of 2π, i.e., when $\Phi^C=2\pi n$. Since $0\le t_a\le 1$ and $0\le t_b\le 1$, this implies that on resonance the total transmission T of the parallel conducting channels given by Eq. (11) is *always* a minimum as a function of Φ^C, irrespective of the transmission probabilities t_a^2 and t_b^2 of the conducting channels, i.e., this model exhibits only resonant reflection, and not resonant transmission. This is true of both Figs. 1(a) and 1(b), since mathemati-

cally these cases are equivalent. The transmission probabilities t_a^2 and t_b^2 and all of the phases in Eq. (14) should vary smoothly with the magnetic field, so that no sudden change of the phase of magnetoconductance oscillations is predicted in these models when t_a^2 and/or t_b^2 passes through any particular value. The crossover from Fig. 1(a) to 1(b) with decreasing t_a and t_b results simply in a broadening of the reflection resonances. This is illustrated in Fig. 2, where T given by (11) is plotted against Φ^C for (a) strong and (b) weak transmission through the parallel channels.

Thus, while these models can account for the existence of magnetoconductance oscillations, they do not explain the interesting details (abrupt phase changes, beats, abrupt period changes) that have recently been observed.

III. INCLUDING MORE EDGE STATES

It is reasonable to ask whether more general scattering models can do better. A model in which both resonant transmission and resonant reflection can occur is shown in Fig. 3.[30] In addition to the edge states L, R, and C shown in Fig. 1(a), another pair of edge states V and W are present and couple to C at d and e.

The analysis in the preceding section can be extended straightforwardly to this case, noting that here the total transmission T through the parallel channels takes the form $T=T_{LL}+T_{WL}+T_{LV}+T_{WV}$, i.e., it consists of terms describing transmission from the edge states entering the system at the upper left in Fig. 3 to those exiting at the lower left. The result is

$$T=1+\frac{t_a^2+t_b^2+t_a^2t_b^2(t_d^2t_e^2-t_e^2-t_d^2)-1}{t_a^2t_b^2t_d^2t_e^2-2t_at_bt_dt_e\cos(\chi^C)+1}\ . \tag{15}$$

Here t_a and t_b are still given by (12) and (13); t_a^2 and t_b^2 are the transmission probabilities of the individual parallel channels. t_d and t_e are defined analogously:

$$t_d=u_{VV}^d=u_{CC}^d\ , \tag{16}$$

$$t_e=u_{WW}^e=u_{CC}^e\ , \tag{17}$$

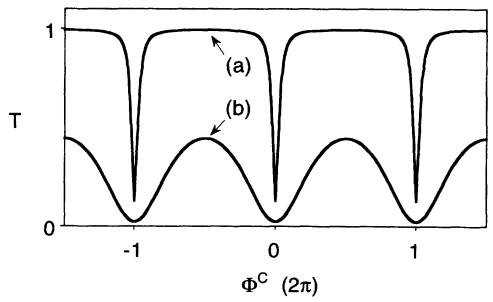

FIG. 2. Examples of the total transmission T of the parallel channels for the models shown in Fig. 1 vs the phase Φ^C accumulated by an electron in going around orbit C. Curve (a) is an example of the case in Fig. 1(a) with individual conducting channels having transmission probabilities $t_a^2=0.8$, $t_b^2=0.9$. Curve (b) is an example of Fig. 1(b) with $t_a^2=0.1$, $t_b^2=0.2$. In each case T is a minimum on resonance ($\Phi^C=2n\pi$), i.e., both curves represent resonant reflection.

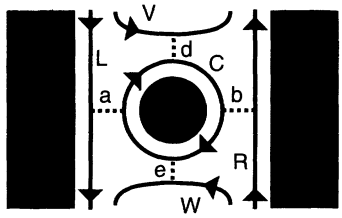

FIG. 3. Model of conduction through a pair of parallel channels similar to Fig. 1(a) but with an additional pair of edge states V and W that couple to the antidot orbit C at d and e.

i.e., t_d^2 is the probability that an electron in edge state V passes through the scattering region d *without* being scattered into edge state C; t_e^2 is the corresponding probability for edge state W. In (15),

$$\chi^C=\varphi_{ae}^C+\theta_{CC}^e+\varphi_{eb}^C+\theta_{CC}^b+\varphi_{bd}^C+\theta_{CC}^d+\varphi_{da}^C+\theta_{CC}^a\ . \tag{18}$$

χ^C is the phase accumulated by an electron in going around the orbit C. Note that as in Eq. (14) for the phase entering the transmission probability in Sec. II only those scattering phase shifts enter (18) which correspond to transmission of an electron along the orbit C. The phases of all of the other elements of the scattering matrices U^a, U^b, U^d, and U^e, were eliminated from the expression for T using the unitarity condition (6). As is the case with Φ^C in Sec. II, χ^C can be thought of intuitively as something resembling an Aharonov-Bohm phase associated with edge state C. On resonance, $\chi^C=2\pi n$ for integer n.

If edge states V and W are decoupled from the antidot orbit C (by setting $t_d=t_e=1$), then Eq. (15) for T reduces to the result (11) of Sec. II, and the system exhibits resonant reflection. However, if C is instead decoupled from L and R ($t_a=t_b=1$), then the total transmission is

$$T'=1+\frac{(1-t_d^2)(1-t_e^2)}{t_d^2t_e^2-2t_dt_e\cos(\chi^C)+1}\ , \tag{19}$$

which is a maximum on resonance, so that the system exhibits resonant transmission. More generally, resonant transmission (reflection) occurs if the numerator of the second term on the right-hand side (RHS) of Eq. (15) is positive (negative). Thus, if the values of t_a, t_b, t_e, and t_d vary with magnetic field, the system can switch *abruptly* from resonant transmission to resonant reflection when the value of the numerator passes through zero. This implies that $T=1$ at the switchover. That is, in this model, the transition from resonant transmission to resonant reflection occurs when the two-terminal conductance of the system is me^2/h, with $m=1$ or 2, depending on whether the system is spin resolved or not.[31]

This is the case in the numerical simulations reported in Ref. 9, where the transition occurs at the $m=2$ conductance plateau. However, since only one Aharnov-Bohm-like phase χ^C appears in the transmission T given by (15), only a single series of resonant spikes (switching over from transmission to reflection) is to be expected in this model, whereas the behavior found numerically in

Ref. 9 is, at least in some cases, more complicated.

The transition from resonant transmission to resonant reflection in this model results in a π phase shift of the conductance oscillations, which is abrupt, happening in a single oscillation. But this is clearly not the explanation of the experimental π phase shifts that have been reported,[14,15] since these were seen at conductance values that are not close to integer multiples of e^2/h.

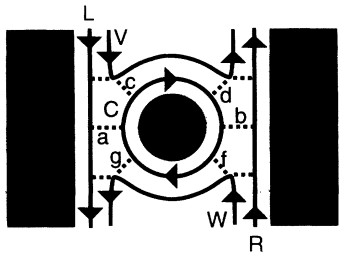

FIG. 4. Model of conduction through a pair of parallel channels with the edge states present similar to those in Fig. 3, but with a different coupling scheme between edge states V, W, and C.

IV. AN IMPROVED EDGE-STATE COUPLING SCHEME

The model discussed in Sec. III is the simplest possible coupling scheme involving the five edge states C, L, R, V, and W. However, as was shown above, it cannot explain the recent experimental data. Here I will discuss another possible coupling scheme between the edge states V and C, and W and C, which may be more realistic. If the mixing between these edge states is due to the geometry of the depletion potential (rather than random defects), then it is reasonable to expect it to be strongest near the openings of the parallel conducting channels, where the potential has the most structure. This suggests the coupling scheme shown in Fig. 4. The scattering events shown between edge-state pairs L and V, L and W, R and V, and R and W, have no effect on the conduction through the parallel channels. This is because these pairs of edge states either originate at a common reservoir before the scattering event, or flow to a common reservoir after the scattering event. On the other hand, the pairs of successive scatterings labeled c and d, and f and g, form interference loops between the pairs of edge states V and C, and W and C, respectively, and can have a strong effect on the conduction. Analogous coupling schemes[25,27] have been successful in describing quantum interference effects that are observed[32,33] in magnetotransport through quantum dots.

The total transmission T through the parallel channels can be found analytically for this model as well. The procedure used is again a direct extension of that described in Sec. II. The result is

$$T=1+\frac{(t_b^2X-r_a^2)F^-(r_dt_c,r_ct_d,\Omega_{VC})-r_a^2r_b^2F^+(r_cr_d,t_ct_d,\Omega_{VC})}{1-2t_at_bY+t_a^2t_b^2F^+(r_cr_d,t_ct_d,\Omega_{VC})F^+(r_fr_g,t_ft_g,\Omega_{WC})}\ , \tag{20}$$

where

$$X=r_a^2F^+(r_fr_g,t_ft_g,\Omega_{WC})+F^-(r_gt_f,r_ft_g,\Omega_{WC})\ , \tag{21}$$

$$Y=r_cr_dG(\Omega_{VW},\Omega_V)+t_ct_dG(\Omega_W,\Omega_C)\ , \tag{22}$$

$$F^{\pm}(a,b,\Omega)=a^2\pm 2ab\cos\Omega+b^2\ , \tag{23}$$

$$G(\Omega_1,\Omega_2)=r_fr_g\cos\Omega_1+t_ft_g\cos\Omega_2\ , \tag{24}$$

$$r_i=\sqrt{1-t_i^2}\ . \tag{25}$$

t_i is defined as in the preceding sections [Eqs. (12), (13), (16), and (17)], so that t_i^2 is the probability of an electron passing through scattering region i without switching to a different edge state. The phases appearing in the above expressions are

$$\Omega_C=\varphi_{ag}^C+\theta_{CC}^g+\varphi_{gf}^C+\theta_{CC}^f+\varphi_{fb}^C+\theta_{CC}^b+\varphi_{bd}^C+\theta_{CC}^d+\varphi_{dc}^C+\theta_{CC}^c+\varphi_{ca}^C+\theta_{CC}^a\ , \tag{26}$$

$$\Omega_V=\varphi_{ag}^C+\theta_{CC}^g+\varphi_{gf}^C+\theta_{CC}^f+\varphi_{fb}^C+\theta_{CC}^b+\varphi_{bd}^C+\theta_{CV}^d+\varphi_{dc}^V+\theta_{VC}^c+\varphi_{ca}^C+\theta_{CC}^a\ , \tag{27}$$

$$\Omega_W=\varphi_{ag}^C+\theta_{CW}^g+\varphi_{gf}^W+\theta_{WC}^f+\varphi_{fb}^C+\theta_{CC}^b+\varphi_{bd}^C+\theta_{CC}^d+\varphi_{dc}^C+\theta_{CC}^c+\varphi_{ca}^C+\theta_{CC}^a\ , \tag{28}$$

with

$$\Omega_{VC}=\Omega_V-\Omega_C\ ,\quad \Omega_{WC}=\Omega_W-\Omega_C$$

and

$$\Omega_{VW}=\Omega_V+\Omega_W-\Omega_C\ .$$

This expression for T is complicated enough that its implications are best studied numerically. Nonetheless, having the analytic result is useful. This is because the effects of the six unitary matrices representing the scattering at a, c, d, b, f, and g in Fig. 4 are expressed in terms of only six real transmission amplitudes t_a, t_c, t_d, t_b, t_f, and t_g, and three phases Ω_C, Ω_V, and Ω_W, which have simple physical meanings: Ω_C is the phase (including the scattering phase shifts) accumulated by an electron in going around the orbit C in Fig. 4. Ω_V is the phase accumulated by going from d to c clockwise along orbit C and completing a closed orbit by crossing from C to V at c, going from c to d along V and returning to C at d. Ω_W is the phase accumulated around the corresponding orbit constructed out of C and the part of W between f and g.

V. IMPLICATIONS OF THE MODEL AND POSSIBLE CONNECTION WITH EXPERIMENTS

I will now discuss the implications of the analytic results presented in Sec. IV, focusing particularly on the

possible relationship between these results and conductance features that have been observed experimentally in two distinct regimes.

A representative plot of the transmission T given by (20) in the low-conductance regime where π phase shifts of the magneto-oscillations of the conductance have been reported[14,15] is shown in Fig. 5. In the plot, the amplitudes t_a, t_c, t_d, t_b, t_f, and t_g are held fixed and the phases Ω_C, Ω_V, and Ω_W are varied, keeping the ratios Ω_V/Ω_C and Ω_W/Ω_C constant. The vertical lines in the plot are a uniformly spaced grid. The transmission T exhibits sharp phase changes of approximately π (similarly to those seen experimentally) at the nodes of the pattern that occur near $\Omega_C=6\times 2\pi$ and $\Omega_C=35\times 2\pi$. However, smaller and more gradual phase changes in the oscillation pattern can also be seen in Fig. 5; these occur wherever the envelope of the oscillations of T with Ω_C narrows. It is unclear whether such slower phase changes are also present in the experimental data. It should be noted that the phase changes visible in Fig. 5 are not due to switching between resonant transmissions and resonant reflection. Rather, they are an interference effect between the different orbits that an electron can take around the antidot in the magnetic field. In the vicinity of the phase changes in Fig. 5, the local period of the oscillations is slightly larger than it is before or after the phase change. The opposite behavior (local compression of the period of the oscillations at a phase change) also occurs in this model in situations where t_c^2 and t_d^2, and/or t_f^2 and t_g^2 are close to 0.5.

Another regime in which experiments have been carried out[16] corresponds to total conductances G above the first (spin unresolved) quantized plateau, i.e., for $G>2e^2/h$. The present model exhibits behavior qualitatively similar to that observed in this regime as well. In this regime, the gates defining the system in the experiments are set so that there is perfect transmission of one mode through each of the two parallel conductors. In the present model this corresponds to $t_a=t_b=1$;[34] the scattering pattern is illustrated in Fig. 6. A representative plot of the transmission T given by (20) in this regime is shown in Fig. 7. Here again the amplitudes t_c, t_d, t_f, and t_g are held fixed and the phases Ω_C, Ω_V, and Ω_W are varied, keeping the ratios Ω_W/Ω_C and Ω_V/Ω_C constant. The beatlike features shown in Fig. 7 are very similar to those observed experimentally.[35] Their origin can be understood as follows: For $t_a=t_b=1$, T given by (20) reduces to

$$T''=1+\frac{F^-(r_g t_f, r_f t_g, \Omega_{WC})F^-(r_d t_c, r_c t_d, \Omega_{VC})}{1-2Y+F^+(r_c r_d, t_c t_d, \Omega_{VC})F^+(r_f r_g, t_f t_g, \Omega_{WC})}. \tag{29}$$

The factors F^- in the numerator of the RHS have minima when $\Omega_{VC}=\Omega_V-\Omega_C$ and $\Omega_{WC}=\Omega_W-\Omega_C$ are equal to integer multiples of 2π, and these minima manifest themselves as the nodes of the beat pattern in Fig. 7 that are marked $\Diamond$ and $+$, respectively, i.e., the beat pattern is due to interference between the orbit C of the antidot, and the two orbits discussed at the end of Sec. IV that are constructed out of C and V and C and W.

This interference effect can be understood intuitively by considering the result

$$\Omega_{WC}=(\theta_{CW}^g+\varphi_{gf}^W+\theta_{WC}^f)-(\theta_{CC}^g+\varphi_{gf}^C+\theta_{CC}^f) \tag{30}$$

that follows from (26) and (28), and the corresponding expression for Ω_{VC}. Consider an electron that has entered edge state C from V in Fig. 6: To be transmitted through the structure it must exit C through edge state W. This

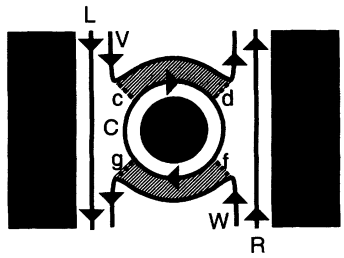

FIG. 6. Model for the case of perfect transmission through the two parallel conducting channels. The hatched areas are the interference loops responsible for the beat pattern in Fig. 7.

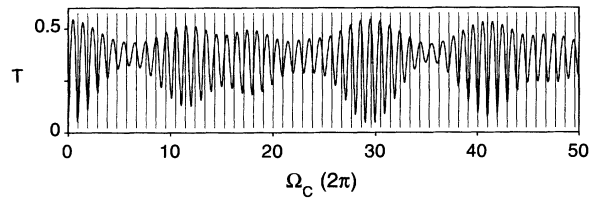

FIG. 5. Total transmission T through the pair of conducting channels calculated for the model in Fig. 4, at low transmission. Ω_C is the phase accumulated by an electron in going around the orbit C of the antidot. Model parameters used are $t_a^2=0.15$, $t_b^2=0.25$, $t_c^2=0.8$, $t_d^2=0.7$, $t_f^2=0.75$, $t_g^2=0.6$, $\Omega_V/\Omega_C=1.1$, and $\Omega_W/\Omega_C=1.07$. The vertical lines are a uniformly spaced grid. Abrupt π phase changes of the transmission oscillations occur at the nodes of the interference pattern near $\Omega_C=6\times 2\pi$ and $\Omega_C=35\times 2\pi$. Slower phase changes not equal to π occur where the oscillation envelope narrows near $\Omega_C=15$, 22, and $50\times 2\pi$.

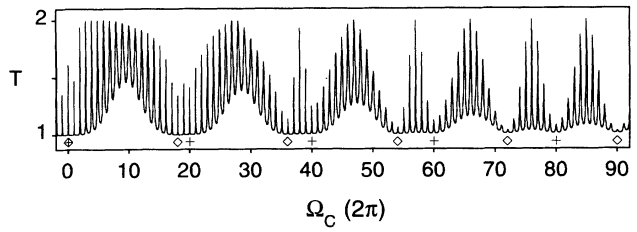

FIG. 7. Total transmission T through the pair of conducting channels calculated for the model in Figs. 4 and 6, for perfect transmission through the channels at a and b. Ω_C is the phase accumulated by an electron in going around the orbit C of the antidot. Model parameters used are $t_a=1.0$, $t_b=1.0$, $t_c^2=0.8$, $t_d^2=0.7$, $t_f^2=0.75$, $t_g^2=0.6$, $\Omega_W/\Omega_C=1\frac{1}{20}$, and $\Omega_V/\Omega_C=1\frac{1}{18}$. The two series of nodes of the beat pattern are marked $\Diamond$ and $+$. They occur where $\Omega_V-\Omega_C$ and $\Omega_W-\Omega_C$ equal integer multiples of 2π, respectively. Their physical meaning is explained in the text.

involves the scattering events f and g. The first set of parentheses on the RHS of Eq. (30) for Ω_{WC} is the total phase that the electron acquires when it scatters from C to W at f, travels from f to g in W, and then scatters back from W to C at g. The second set of parentheses is the phase that the electron acquires if it stays in C at f, travels from f to g in C, and then stays in C at g, i.e., Ω_{WC} is the difference in phase between the two paths that an electron can take around the shaded region at the bottom of Fig. 6. When this difference is an integer multiple of 2π, there is constructive interference, and transmission from C to C via f and g is enhanced. Correspondingly, transmission from C to W via f and g is suppressed. Thus T is reduced, and a node occurs in Fig. 7. The shaded region between C and V in Fig. 6 has a similar role.

An analogous interference mechanism[25] has been successful in describing quantum Hall anomalies that are observed[32] in quantum dots. Those anomalies are known to persist to temperatures that are unusually high for mesoscopic interference phenomena, up to several kelvin. Thus, it is interesting to consider whether the node-antinode structure of the beat pattern in the present antidot system should be similarly robust to temperature. This appears to be the case experimentally.[36] To calculate the temperature T^* at which kT smearing of the Fermi function would be expected to destroy the beat pattern, it is necessary to know the energy dependence of the phase differences Ω_{VC} and Ω_{WC} at fixed magnetic field. A complete treatment of this problem would require elaborate numerical calculations and is beyond the scope of this paper. However, a simple estimate can be obtained by modeling the parts of C and V between c and d (and the corresponding parts of C and W) as portions of the innermost and next-to-innermost edge states of an isolated azimuthally symmetric antidot, respectively. These eigenstates are of the form $\Psi_{ln}=e^{il\phi}R_{ln}(r)$ where r and ϕ are the radial and azimuthal coordinates. Then, neglecting the energy dependence of the scattering phase shifts θ^i_{XY} that appear in Ω_{VC} and Ω_{WC}, one can estimate the temperature at which the beat pattern should disappear as

$$kT^* \approx \xi \left| \frac{\partial}{\partial \varepsilon}(l_1 - l_2) \right|^{-1}, \tag{31}$$

where l_1 and l_2 are the azimuthal eigenvalues l of the innermost and next-to-innermost edge states, respectively, at the Fermi energy ε, and ξ is a geometrical factor close to unity. The l_i need to be calculated as a function of the energy ε, in order to evaluate (31). A convenient numerical procedure for this is described in Ref. 37. Applying it here yields $T^* \sim 5$ K at $B=2$ T for a 400-nm-diameter antidot in a two-dimensional electron gas in GaAs and $\varepsilon=7.15$ meV. Equation (31) also implies that T^* decreases with increasing B or decreasing ε, because $|\partial l_2/\partial \varepsilon|$ becomes large as the second-lowest Landau level depopulates. In fact, when the Fermi level coincides with the second bulk Landau level, the second edge mode of the antidot at the Fermi energy becomes a bulk state and is then dispersionless, so that $|\partial l_2/\partial \varepsilon|$ diverges. The rapid decrease of T^* with increasing B predicted by this argument is in qualitative agreement with the results of recent measurements.[36] However, the values of T^* estimated in this way are somewhat larger than the experimentally observed smearing temperatures.[36] This suggests that inelastic scattering also may play a significant role in smearing out the beat pattern as the temperature increases, as is the case with the related quantum Hall anomalies in quantum dot systems.[25,32]

VI. CONCLUSIONS

It has been shown above that the scattering model described in Sec. IV is able to account qualitatively for some key features of the experimental data at low and moderate magnetic fields. These features are abrupt phase changes of the magneto-oscillations of the conductance at conductance values $G < 2e^2/h$ (spin unresolved),[14,15] and beatlike conductance structures at $G > 2e^2/h$.[16] However, this model does not account for abrupt increases of the period of the conductance oscillations that are observed to occur with increasing magnetic field in the $G > 2e^2/h$ regime.[16] These period jumps can be explained[16] in terms of a different mechanism, namely, edge-state formation at random variations of the potential in the vicinity of the antidot. Experimentally, the period changes are often accompanied by abrupt phase changes of the conductance oscillations.[16] Thus, it appears that in addition to the mechanism discussed in this paper, there is at least one other (quite different) way in which abrupt phase changes can be generated. In view of this, it may be significant that π phase changes at low conductance have been reported also at high magnetic fields ($B \sim 9$ T) in the spin-resolved regime where only the lowest spatial Landau level is populated.[15] In this regime, the edge states V and W in Fig. 4 have the opposite spin to that of edge states L, C, and R, and thus an explanation of π phase changes within the present scattering model would require spin-flip scattering. It is not clear whether this requirement is satisfied by the experimental system. On the other hand, edge-state formation at potential irregularities is certainly possible under these conditions. Further experimental and theoretical studies of these effects will clearly be of interest.

ACKNOWLEDGMENTS

I wish to thank A. S. Sachrajda for many stimulating discussions, C. J. B. Ford for helpful correspondence, and C. Dharma-wardana, P. T. Coleridge, and E. Fenton for their comments.

*Present address.

[1]B. J. van Wees, H. van Houten, C. W. J. Beenakker, J. G. Williamson, L. P. Kouvenhoven, D. van der Marel, and C. T. Foxon, Phys Rev. Lett. **60**, 848 (1988); D. A. Wharam, M. Pepper, H. Ahmed, J. E. F. Frost, D. G. Hasko, D. C. Peacock, D. A. Ritchie, and G. A. C. Jones, J. Phys. C **21**, L209 (1988).

[2]Y. Imry, in *Directions in Condensed Matter Physics,* edited by G. Grinstein and G. Mazenko (World Scientific, Singapore, 1986), Vol. 1; G. Kirczenow, Phys. Rev. B **38**, 10958 (1988); Solid State Commun. **68**, 715 (1988); L. I. Glazman, G. B. Lesovick, D. E. Khmelnitskii, and R. I. Shekhter, Pis'ma Zh. Eksp. Teor. Fiz. **48**, 218 (1988) [JETP Lett. **48**, 238 (1988)]; Y. B. Levinson, *ibid.* **48**, 273 (1988) [**48**, 301 (1988)]; A. Szafer and A. D. Stone, Phys. Rev. Lett. **48**, 301 (1988); E. Haanappel and D. van der Marel, Phys. Rev. B **39**, 5484 (1989); G. Kirczenow, J. Phys. Condens. Matter **1**, 305 (1989); L. Escapa and S. Garcia, *ibid.* **1**, 2125 (1989); E. Tekman and S. Ciraci, Phys. Rev. B **39**, 8772 (1989); G. Kirczenow, *ibid.* **39**, 10452 (1989); S. He and S. Das Sarma, *ibid.* **40**, 3379 (1989); Y. Avishai and Y. Band, *ibid.* **40**, 3429 (1989); A. Kawabata, J. Phys. Soc. Jpn. **58**, 372 (1989); M. Büttiker, Phys. Rev. B **41**, 7906 (1990); E. Castaño and G. Kirczenow, *ibid.* **45**, 1514 (1992); D. L. Maslov, C. Barnes, and G. Kirczenow, Phys. Rev. Lett. **70**, 2543 (1993); Phys. Rev. B **48**, 2543 (1993).

[3]For a review see S. E. Ulloa, A. MacKinnon, E. Castaño, and G. Kirczenow, in *Handbook on Semiconductors,* edited by T. S. Moss and P. T. Landsberg (Elsevier, New York, 1992), Vol. 1, p. 863.

[4]C. G. Smith, M. Pepper, R. Newbury, H. Ahmed, D. G. Hasko, D. C. Peacock, J. E. F. Frost, D. A. Ritchie, G. A. C. Jones, and G. Hill, J. Phys. Condens. Matter **1**, 6763 (1989).

[5]J. A. Simmons, H. P. Wei, L. W. Engel, D. C. Tsui, and M. Shayagan, Phys. Rev. Lett. **63**, 1731 (1989).

[6]Y. Hirayama and T. Saku, Phys. Rev. B **42**, 11408 (1990); Jpn. J. Appl. Phys. **29**, L368 (1990).

[7]Y. Avishai, M. Kaveh, S. Shatz, and Y. Band, J. Phys Condens. Matter **1**, 6907 (1989).

[8]E. Castaño and G. Kirczenow, Phys. Rev. B **41**, 5055 (1990).

[9]Y. Takagaki and D. K. Ferry, Surf. Sci. **305**, 669 (1994).

[10]Y. Sun and G. Kirczenow, Phys. Rev. Lett. **72**, 2450 (1994).

[11]P. J. Simpson, D. R. Mace, C. J. B. Ford, I. Zailer, M. Pepper, D. A. Ritchie, J. E. F. Frost, M. P. Grimshaw, and G. A. C. Jones, Appl. Phys. Lett. **63**, 3191 (1993).

[12]Y. Aharonov and D. Bohm, Phys. Rev. **115**, 485 (1959).

[13]Y. Feng, A. S. Sachrajda, R. P. Taylor, J. A. Adams, M. Davies, P. Zawadzki, P. T. Coleridge, P. A. Marshall, and R. Barber, Appl. Phys. Lett. **63**, 1666 (1993).

[14]P. J. Simpson, C. J. B. Ford, D. R. Mace, I. Zailer, M. Josefin, M. Pepper, D. A. Ritchie, J. E. Frost, and G. A. C. Jones, Surf. Sci. **305**, 453 (1994).

[15]C. J. B. Ford, P. J. Simpson, I. Zailer, D. R. Mace, M. Yosefin, M. Pepper, D. A. Ritchie, J. E. Frost, M. P. Grimshaw, and G. A. C. Jones (unpublished).

[16]G. Kirczenow, A. S. Sachrajda, Y. Feng, R. P. Taylor, L. Henning, J. Wang, P. Zawadzki, and P. T. Coleridge, Phys. Rev. Lett. **72**, 2069 (1994).

[17]For a review of the Coulomb blockade see M. A. Kastner, Rev. Mod. Phys. **64**, 849 (1992).

[18]P. A. Lee and D. S. Fisher, Phys Rev. Lett. **47**, 882 (1981).

[19]A. MacKinnon, Z. Phys. B **59**, 385 (1985).

[20]B. I. Halperin, Phys. Rev. B **25**, 2185 (1982).

[21]A. D. Stone and A. Szafer, IBM J. Res. Dev. **32**, 384 (1988).

[22]M. Büttiker, Phys. Rev. B **38**, 12724 (1988).

[23]G. Kirczenow, Phys. Rev. B **42**, 5357 (1990).

[24]M. Büttiker, Semicond. Semimet. **35**, 191 (1992).

[25]G. Kirczenow and E. Castaño, Phys. Rev. B **43**, 7343 (1991).

[26]G. Kirczenow, Surf. Sci. **263**, 330 (1992); Phys. Rev. B **46**, 1439 (1992); B. L. Johnson and G. Kirczenow, Phys. Rev. Lett. **69**, 672 (1992); B. L. Johnson, C. Barnes, and G. Kirczenow, Phys. Rev. B **46**, 15302 (1992); C. Barnes, B. L. Johnson, and G. Kirczenow, Phys. Rev. Lett. **70**, 115 (1993); R. Akis, C. Barnes, B. L. Johnson, and G. Kirczenow, Phys. Rev. B **47**, 16382 (1993).

[27]C. Barnes, R. P. Taylor, A. S. Sachrajda, and T. Sugano (unpublished).

[28]A brief summary of some of the present results has been presented in Ref. 16.

[29]The expression [Eq. (11)] for the total transmission probability T of the parallel conducting channels obtained here is equivalent to expressions given by Büttiker (Ref. 24) describing a two-terminal conductor with a localized resonant state. The derivation outlined here is given in order to establish the notation and the method to be used in the more complicated cases considered in the remainder of this paper.

[30]This model was discussed in Ref. 9, but without its analytic solution, which is given here.

[31]For general reviews of the relationships between transmission coefficients and conductances that have been developed since the issue was first addressed by Landauer [R. Landauer, IBM J. Res. Dev. **1**, 223 (1957)], see Imry in Ref. 2 and also see Ref. 3.

[32]C. J. B. Ford, S. Washburn, R. Newbury, C. M. Knoedler, and J. M. Hong, Phys. Rev. B **43**, 7339 (1991).

[33]R. P. Taylor, A. S. Sachrajda, P. Zawadzki, P. T. Coleridge, and J. A. Adams, Phys. Rev. Lett. **69**, 1989 (1992); A. S. Sachrajda, R. P. Taylor, C. Dharma-wardana, P. Zawadzki, J. A. Adams, and P. T. Coleridge, Phys. Rev. B **47**, 6811 (1993).

[34]Note that if instead one conductor is completely pinched off and the other transmits one mode perfectly, for example, $t_a=1$ and $t_b=0$, then the total transmission of the system as given by the present model [Eq. (20)] is $T=1$, i.e., the total conductance is $G=2e^2/h$ if the system is spin unresolved. This is true for arbitrary phases Ω_C, Ω_V, and Ω_W and arbitrary values of the coupling parameters t_c, t_d, t_f, and t_g between the edge states C, V, and W, and is a consequence of the unitarity of the scattering matrices; the coupling between these edge states has *no* effect on the conductance. Thus, the model is able to describe the conductance quantization that is observed (Ref. 16) when only one of the parallel conducting channels is open. However, if *both* channels are open, the coupling between the edge states C, V, and W can have a very strong effect on the total conductance.

[35]A direct comparison of the results of the model, for reasonable values of the model parameters, with experimental data is given in Ref. 16.

[36]A. S. Sachrajda (private communication).

[37]Y Avishai, Y. Hatsugai, and M. Kohmoto, Phys. Rev. B **47**, 9501 (1993).

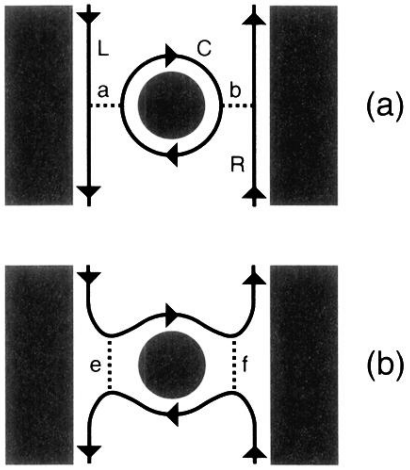

FIG. 1. The simplest models of a pair of parallel conducting channels. There is only a single participating magnetic edge state (solid line) at each boundary between the electron gas (white) and depleted regions (black). Dashed lines denote scattering between different edge states. The electric current flows between reservoirs located at the top and bottom of each figure. (a) the edge states are transmitted through the conducting channels, with some reflection occurring due to mixing between edge states at *a* and *b*. (b) The edge states are reflected at the mouths of the conducting channels, with some transmission occurring due to mixing at *e* and *f*.

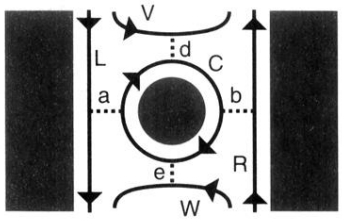

FIG. 3. Model of conduction through a pair of parallel channels similar to Fig. 1(a) but with an additional pair of edge states V and W that couple to the antidot orbit C at d and e.

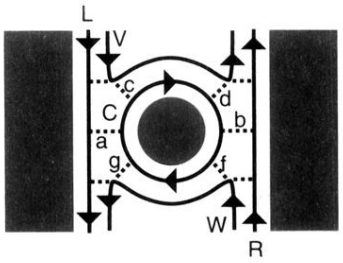

FIG. 4. Model of conduction through a pair of parallel channels with the edge states present similar to those in Fig. 3, but with a different coupling scheme between edge states *V*, *W*, and *C*.

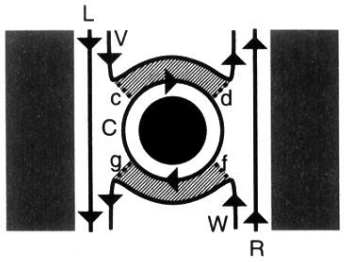

FIG. 6. Model for the case of perfect transmission through the two parallel conducting channels. The hatched areas are the interference loops responsible for the beat pattern in Fig. 7.